interpositus, and very small lesions in this region of the red nucleus also abolish the CR with no effect on the UR (*9, 18*). In trained animals, lidocaine or cold-probe inactivation of the interpositus abolishes both the behavioral CR and the learning-induced neuronal model in the red nucleus; inactivation of the red nucleus abolishes the behavioral CR but has no effect on the learning-induced neuronal model in the interpositus (*14, 20*). Our results demonstrate that the memory trace must be formed at or beyond the cerebellar site of inactivation but before the red nucleus. On the basis of these results and data cited (*15*), we conclude that the memory trace for eyeblink conditioning must be localized to the ipsilateral lateral cerebellum. Our findings strongly support the hypothesis that the memory traces for learned movements are formed and stored in the cerebellum (*21*).

REFERENCES AND NOTES

1. J. H. Byrne, *Physiol. Rev.* **67**, 329 (1987); D. G. Lavond, J. J. Kim, R. F. Thompson, *Annu. Rev. Psychol.*, in press.
2. R. F. Thompson, *Science* **233**, 941 (1986).
3. R. D. Hawkins, G. A. Clark, E. R. Kandel, in *Handbook of Physiology*, F. Plum, Ed. (American Physiological Society, Bethesda, MD, 1987), vol. 5, pp. 25–83; L. R. Squire, *Memory and Brain* (Oxford Univ. Press, New York, 1987).
4. R. R. Matsumoto, *Brain Res. Rev.* **14**, 203 (1989).
5. J. Van-Neerven, O. Pompeiano, H. Collewijn, *Arch. Ital. Biol.* **127**, 243 (1989); J. G. Keating and W. T. Thach, *Soc. Neurosci. Abstr.* **17**, 1381 (1991); J. W. Mink and W. T. Thach, *J. Neurophysiol.* **65**, 330 (1991).
6. J. H. Martin and C. Ghez, *Behav. Brain Res.* **28**, 217 (1988).
7. N. H. Donegan, R. W. Lowry, R. F. Thompson, *Soc. Neurosci. Abstr.* **9**, 331 (1983); T. J. Voneida, *ibid.* **16**, 270 (1990).
8. J. E. Steinmetz *et al.*, *Proc. Natl. Acad. Sci. U.S.A.* **84**, 3531 (1987); J. L. Lewis, J. J. LoTurco, P. R. Solomon, *Behav. Neurosci.* **101**, 151 (1987); D. A. McCormick, J. E. Steinmetz, R. F. Thompson, *Brain Res.* **359**, 120 (1985); M. D. Mauk, J. E. Steinmetz, R. F. Thompson, *Proc. Natl. Acad. Sci. U.S.A.* **83**, 5349 (1986); G. A. Clark, D. A. McCormick, D. G. Lavond, R. F. Thompson, *Brain Res.* **291**, 125 (1984); C. H. Yeo, M. J. Hardiman, M. Glickstein, *Exp. Brain Res.* **60**, 87 (1985); J. E. Steinmetz, D. G. Lavond, D. Ivkovich, C. G. Logan, R. F. Thompson, *J. Neurosci.* **12**, 4403 (1992); J. F. Disterhoft, K. J. Quinn, C. Weiss, M. T. Shipley, *ibid.* **5**, 941 (1985).
9. M. E. Rosenfield, A. Dovydaitis, J. W. Moore, *Physiol. Behav.* **34**, 751 (1983); M. E. Rosenfield and J. W. Moore, *Behav. Brain Res.* **10**, 393 (1983); *ibid.* **17**, 77 (1985).
10. R. H. Lye, D. J. O'Boyle, R. T. Ramsden, W. Schady, *J. Physiol. (London)* **403**, 58P (1988).
11. Details of the surgical cannula implant procedures and behavioral recording apparatus have been published (*20*). Surgical anesthesia was ketamine (60 mg per kilogram of body weight), xylazine (8 mg/kg), and halothane (1 to 3% in oxygen). Each training session consisted of 100 trials: 80 paired trials with 10 tone-alone and 10 airpuff-alone test trials evenly distributed throughout the session. Intertrial intervals ranged between 20 to 40 s (mean, 30 s). Behavioral responses were recorded with a minitorque potentiometer attached to the animal's nictitating membrane by means of surgical suture. A CR was defined as a response greater than 0.5 mm after the CS onset but preceding the US onset.
12. Infusion doses were (i) cerebellar muscimol, 14 nmol in 1 μl of saline vehicle (pH adjusted to 7.4); (ii) saline controls, 1 μl of saline vehicle; or (iii) red nucleus muscimol, 1.3 nmol in 0.75 μl of saline vehicle. All infusion rates were 0.3 μl per minute. The cerebellar muscimol dose was chosen on the basis of previous work to reliably label both the interpositus-dentate nucleus and overlying cerebellar cortex; this dose had no observable behavioral effect on any animal. Likewise, the red nucleus dose was chosen to reliably label the nucleus with minimal spread to other regions. With this dose, some of the animals displayed a slight head tilt to the side contralateral to the infusion and a tendency to walk in a circular direction contralateral to infusion. This effect disappeared within 3 to 4 hours of infusion. All other observable behaviors (for example, grooming, feeding, exploration) were unaffected. Although the cerebellar dose used in this study was greater than the red nucleus dose, we have also trained five rabbits with much lower doses (0.7 nmol) in the cerebellum with identical results.
13. Analysis of variance of UR amplitudes revealed no significant differences between muscimol and saline infusion groups across the 6 days of training during infusion on either paired [$F(2,15) = 0.13$; not significant] or airpuff-alone trials [$F(2,15) = 0.01$; not significant].
14. R. E. Clark and D. G. Lavond, *Behav. Neurosci.* **107**, 264 (1993); R. E. Clark, A. A. Zhang, D. G. Lavond, *ibid.* **106**, 879 (1992).
15. A. F. Nordholm *et al.*, *ibid.*, in press. Continuous lidocaine infusion into the same cerebellar locus as muscimol completely prevented learning in naïve animals. Infusion into white matter ventral to the interpositus (output) prevented expression of CRs, but the naïve animals fully learned the CR, as evidenced in postinfusion training, which suggests that learning occurs when the output of the interpositus to its target sites is blocked.
16. J. P. Welsh and J. A. Harvey, *J. Physiol. (London)* **444**, 459 (1991). Their animals were already well trained to a light CS. They reported subsequent transfer of training to a tone CS during cerebellar lidocaine infusions; their saline controls also showed substantial transfer. In addition, cannulae placements may be critically important (*15*).
17. D. A. McCormick and R. F. Thompson, *J. Neurosci.* **4**, 2811 (1984).
18. P. F. Chapman, J. E. Steinmetz, R. F. Thompson, *Brain Res.* **442**, 97 (1988); D. A. McCormick and R. F. Thompson, *Science* **223**, 296 (1984).
19. D. A. McCormick, P. E. Guyer, R. F. Thompson, *Brain Res.* **245**, 347 (1982).
20. P. F. Chapman, J. E. Steinmetz, L. L. Sears, R. F. Thompson, *ibid.* **537**, 149 (1990).
21. J. S. Albus, *Math. Biosci.* **10**, 25 (1971); J. C. Eccles, *Brain Res.* **127**, 327 (1977); M. Ito, *The Cerebellum and Neural Control* (Raven, New York, 1984); D. Marr, *J. Physiol. (London)* **202**, 437 (1969); W. T. Thach, H. G. Goodkin, J. G. Keating, *Annu. Rev. Neurosci.* **15**, 403 (1992).

22. We thank E. Knudsen for suggestions, M. Baudry and L. Swanson for comments on this manuscript, and C. Logan for assistance throughout this study. Supported by National Institute on Aging grant AG05142, Office of Naval Research contract N00014-91-J-0112, and grants from NSF (BNS-8117115) and the McKnight Foundation (R.F.T.).

15 October 1992; accepted 29 January 1993

Induction of $G\alpha_{i2}$-Specific Antisense RNA in Vivo Inhibits Neonatal Growth

Christopher M. Moxham,* Yaacov Hod, Craig C. Malbon

Guanosine triphosphate-binding regulatory proteins (G proteins) are key elements in transmembrane signaling and have been implicated as regulators of more complex biological processes such as differentiation and development. The G protein $G\alpha_{i2}$ is capable of mediating the inhibitory control of adenylylcyclase and regulates stem cell differentiation to primitive endoderm. Here an antisense RNA to $G\alpha_{i2}$ was expressed in a hybrid RNA construct whose expression was both tissue-specific and induced at birth. Transgenic mice in which the antisense construct was expressed displayed a lack of normal development in targeted organs that correlated with the absence of $G\alpha_{i2}$. The loss of $G\alpha_{i2}$ expression in adipose tissue of the transgenic mice was correlated with a rise in basal levels of adenosine 3′,5′-monophosphate (cAMP) and the loss of receptor-mediated inhibition of adenylylcyclase. These data expand our understanding of G protein function in vivo and demonstrate the necessity for $G\alpha_{i2}$ in the development of liver and fat.

G proteins propagate signals from cell surface receptors to a diverse group of effectors that includes adenylylcyclase, phospholipase C, and cation channels (*1–4*). Visual transduction, neuronal signaling, cell growth and differentiation, and metabolic pathways such as glycogenolysis and gluconeogenesis are mediated by way of G proteins. The G protein $G\alpha_{i2}$ has been implicated in the inhibition of adenylylcyclase and oncogenesis (*5–7*). In order to suppress $G\alpha_{i2}$ expression in vivo, we adopted the use of a construct to express $G\alpha_{i2}$-specific antisense RNA instead of gene disruption. To enhance the accumulation of the $G\alpha_{i2}$ antisense RNA, the target sequence was inserted in the 5′-untranslated region of the rat *phosphoenolpyruvate carboxykinase* (*PEPCK*) gene. The *PEPCK* gene was selected for three reasons. (i) The 2.8-kb hybrid *PEPCK*-$G\alpha_{i2}$ antisense RNA would be more stable than a comparatively short-lived an-

C. M. Moxham and C. C. Malbon, Diabetes and Metabolic Diseases Research Program, Department of Molecular Pharmacology, Health Sciences Center, State University of New York (SUNY)/Stony Brook, Stony Brook, NY 11794-8651.
Y. Hod, Department of Physiology and Biophysics, Health Sciences Center, SUNY/Stony Brook, Stony Brook, NY 11794-8661.

*To whom correspondence should be addressed.

tisense RNA oligonucleotide. (ii) Because *PEPCK* expression is regulated by several hormones including glucagon (acting by way of cAMP), glucocorticoids, thyroid hormone, and insulin, the insertion of the antisense sequence within the *PEPCK* gene would confer regulated expression of the antisense sequence. Cyclic AMP coordinately increases the transcription rate of the *PEPCK* gene and the stability of the *PEPCK* mRNA (*8, 9*). (iii) Most importantly, expression of the *PEPCK* gene is developmentally regulated; transcription of the gene initiates at birth (*10, 11*). Thus, expression of the $G\alpha_{i2}$ antisense RNA after birth would prevent any potentially lethal outcome from the suppression of $G\alpha_{i2}$ in utero.

The utility of the construct for the expression of the $G\alpha_{i2}$ antisense RNA within the *PEPCK* gene (pPCK-ASGα_{i2}, Fig. 1) was evaluated first after transfection into FTO-2B rat hepatoma cells. Wild-type FTO-2B cells display cAMP-inducible *PEPCK* gene expression (*8*) and express $G\alpha_{i2}$. RNA antisense to $G\alpha_{i2}$ was detected in FTO-2B clones transfected with pPCK-ASGα_{i2} after reverse transcription of total cellular RNA followed by polymerase chain reaction (PCR) amplification (*12*). FTO-2B clones transfected with pPCK-ASGα_{i2} displayed normal amounts of $G\alpha_{i2}$ expression in the absence of cAMP, an inducer of *PEPCK* gene expression (*13*). $G\alpha_{i2}$ expression declined >85% when the same cells were challenged with the cAMP analog, 8-(4-chlorphenylthio)–cAMP (CPT-cAMP) for 12 days (*13*). FTO-2B clones transfected with the control vector lacking the antisense sequence to $G\alpha_{i2}$ displayed no change in $G\alpha_{i2}$ expression. In contrast to the suppression of $G\alpha_{i2}$, the steady-state amounts of $G\alpha_s$ and $G\alpha_{i3}$ were not changed in cells expressing the RNA antisense to $G\alpha_{i2}$ (*13*), demonstrating that the effect of the antisense RNA expression was specific for $G\alpha_{i2}$. The time elapsing between the induction of pPCK-ASGα_{i2} by CPT-cAMP and the decline of steady-state amounts of $G\alpha_{i2}$ likely reflects the half-life of this subunit, reported to be ~3 days (*14*).

$G\alpha_{i2}$ is the member of the G_i family most prominently implicated in mediating the inhibitory adenylylcyclase pathway. Suppression of $G\alpha_{i2}$ expression in FTO-2B cells was associated with the loss of receptor-mediated inhibition of adenylylcyclase (Fig. 2, A and B). Inhibition of forskolin-stimulated cAMP accumulation by either somatostatin (Fig. 2A) or the A1-purinergic agonist (−)-N^6-(R-phenylisopropyl)-adenosine (R-PIA, Fig. 2B) was nearly abolished in transfectant cells in which RNA antisense to $G\alpha_{i2}$ was first induced by CPT-cAMP for 12 days. Cells transfected with the vector lacking the antisense sequence for $G\alpha_{i2}$ displayed a normal inhibitory adenylylcyclase response following a 12-day challenge with CPT-cAMP. These data demonstrate that $G\alpha_{i2}$ mediates the hormonal inhibition of hepatic adenylylcyclase.

Because the pPCK-ASGα_{i2} construct reduced $G\alpha_{i2}$ subunit expression in vitro, we expanded this approach to in vivo studies to explore the consequences of $G\alpha_{i2}$ antisense RNA expression in transgenic mice. BDF1 mice carrying the *pPCK-ASG*α_{i2} transgene were identified by DNA (Southern) analysis (Fig. 3). Four founder lines were bred and characterized over four generations. Necropsy and histology of the transgenic and control mice were performed. Whereas epididymal fat mass was 0.27 ± 0.01 g in control mice, it was only 0.09 ± 0.03 g in transgenic mice; a 65% decrease in fat mass after 6 weeks of neonatal growth and antisense RNA expression (Table 1). By 18 weeks of age, fat mass had increased in all mice, but the transgenic mice still displayed a ~60% reduction. The pPCK-ASGα_{i2} transgenic mice also displayed a 30% reduction in liver

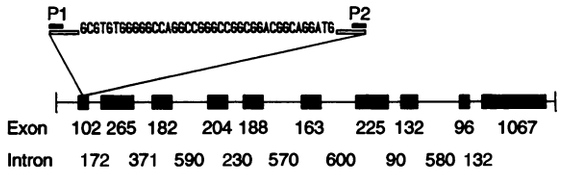

Fig. 1. The pPCK-ASGα_{i2} construct designed for inducible antisense RNA production. The 39 nucleotides immediately upstream and including the translation initiation codon were selected as the $G\alpha_{i2}$ antisense sequence because of the low degree of homology with other G protein α subunits. This sequence did not show significant homology with any of the sequences present in the GenBank database. The construction is described (*20*).

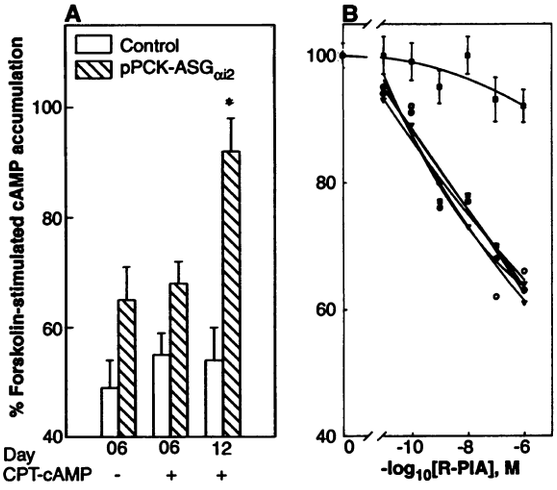

Fig. 2. Antisense RNA-induced loss in $G\alpha_{i2}$ expression reduces hormonal inhibition of adenylylcyclase. Cells were treated with the indicated agonists for 15 min at 37°C. The reaction was terminated with HCl (0.1 N final) and heating to 100°C. The amount of cAMP generated was determined with the use of a competitive binding assay (*21*). (**A**) Somatostatin inhibition of adenylylcyclase in cells transfected with the control vector or the pPCK-ASGα_{i2} construct challenged with CPT-cAMP for 6 or 12 days. (**B**) R-PIA dose response. Cells transfected with the control vector (open symbols) or the pPCK-ASGα_{i2} construct (solid symbols) were incubated with increasing concentrations of R-PIA. Dose response curves were generated from cells cultured either in the absence (○, ●) or the presence of CPT-cAMP for 6 days (△, ▲) or 12 days (□, ■). The values reported are from three separate experiments performed in triplicate and are expressed as mean ± SEM.

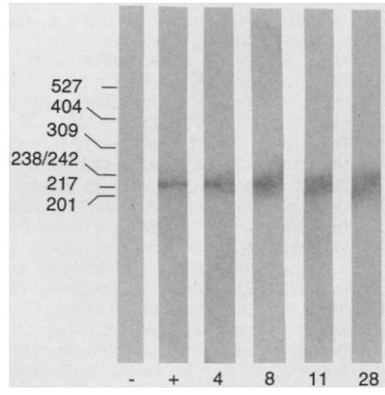

Fig. 3. Identification of pPCK-ASGα_{i2} transgenic mice. The pPCK-ASGα_{i2} construct was excised as a 7.0-kb Eco RI–Bam HI fragment free of vector sequences and microinjected into single cell, preimplantation embryos and then the microinjected embryos were transferred into pseudopregnant recipients. Mouse tail biopsies were obtained from the offspring and genomic DNA was isolated (*22*). Of the 30 offspring, four mice were positive for the pPCK-ASGα_{i2} transgene by dot-blot analysis (*23*). To confirm these results, DNA from the positive mice was subjected to PCR amplification (*24*) with the primers shown in Fig. 1 and then used in Southern analysis. The PCR reaction products were separated by 4% agarose gel electrophoresis, transferred to nylon membranes, and hybridized at 65°C with a random-primed pLNC-ASGα_{i2} plasmid labeled with [^{32}P]dATP according to the manufacturer's protocols (Stratagene). The appearance of a [^{32}P]labeled, 0.23-kb band indicated the animal was transgenic. Lanes labeled from left to right are − (BDF1 mouse tail DNA as negative control), + (pPCK-ASGα_{i2} plasmid as positive control), and mouse lines 4, 8, 11, and 28.

mass at 6 and at 18 weeks of age (Table 1). Inspection of a wider range of tissues and organs (Table 1) indicated that growth had been diminished in tissues selectively targeted for *pPCK-ASG*α_{i2} gene expression (that is, in tissues which normally express *PEPCK*). The growth of brain, heart, lung, and skeletal muscle was unaffected in mice containing the *pPCK-ASG*α_{i2} transgene. Kidney development was unilateral in two transgenic mice and prominent vacuolation localized to the proximal convoluted tubule of the kidney cortex was observed in 30% of all other transgenic mice. Kidney mass on average, however, was not appreciably altered. The basis for the appearance of the vacuoles and a determination of their contents will require further analysis.

With the use of a probe designed to simultaneously detect and discriminate between both the *pPCK-ASG*α_{i2} RNA and the endogenous *PEPCK* mRNA in a ribonuclease (RNAase) protection assay, we detected the endogenous *PEPCK* mRNA but were unable to detect the *pPCK-ASG*α_{i2} RNA expression in either FTO-2B cells stably transfected with the pPCK-ASGα_{i2} construct or in target tissues of pPCK-ASGα_{i2} transgenic mice (*15*). In the transgenic mice, the amount of endogenous *PEPCK* mRNA in hepatic and adipose tissue was elevated compared to the controls. In RNAase protection assays, the endogenous *PEPCK* mRNA was shown to be induced after challenge with CPT-cAMP in FTO-2B cells stably transfected with either the control vector or the pPCK-ASGα_{i2} construct. With reverse transcription and subsequent PCR amplification of liver RNA samples which provided greater sensitivity, we were able to detect antisense RNA expression in the liver of the transgenic mice (Fig. 4). This PCR product comigrated with the product of the reverse transcription and PCR amplification reaction of pPCK-ASGα_{i2} RNA, the positive control (Fig. 4). In contrast to the products obtained from the hepatic RNA of transgenic mice, reaction products of the reverse transcription and PCR amplification of the liver RNA samples from the BDF1 control mice did not display a product with this mobility (Fig. 4).

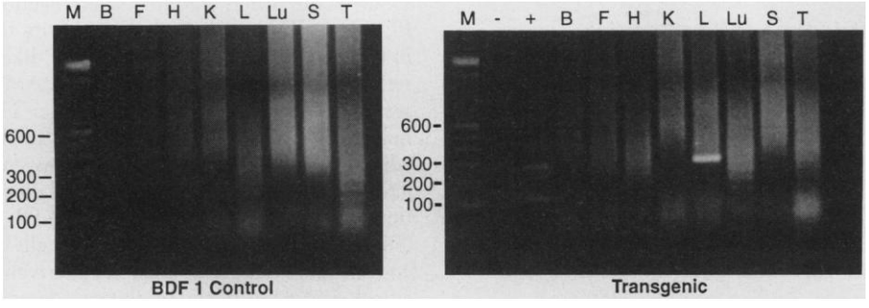

Fig. 4. Detection of pPCK-ASGα_{i2} RNA expression. The indicated tissues were isolated from control and transgenic mice and total RNA was extracted. One microgram of total RNA was reverse-transcribed according to the manufacturer's protocol (Promega) with the pPCK-ASGα_{i2}–specific downstream primer, P2, to prime the reverse transcription. The reverse transcription products were then PCR-amplified with the primers P1 and P2 under the following conditions for 50 cycles: 95°C, 1 min; 60°C, 1 min; 72°C, 2 min. The reaction products were loaded onto a 2% agarose gel and visualized by staining with ethidium bromide. Left: Total RNA isolated from BDF1 control mice. Lanes labeled from left to right are M, 100-bp DNA ladder (Gibco BRL); B, brain; F, fat; H, heart; K, kidney; L, liver; Lu, lung; S, spleen; and T, testes. Right: Total RNA isolated from pPCK-ASGα_{i2} transgenic mice. Lanes labeled from left to right are M, 100-bp DNA ladder (Gibco BRL); –, negative control; +, positive control RNA (pPCK-ASGα_{i2} DNA transcribed in vitro); B, brain; F, fat; H, heart; K, kidney; L, liver; Lu, lung; S, spleen; and T, testes.

Each of the founder mice and their transgenic offspring displayed sharply reduced Gα_{i2} expression in fat, liver, and in some cases kidney (Fig. 5A); tissues in which the *PEPCK* gene is expressed. The amount of Gα_{i2} expression was equivalent to wild type in brain, lung, spleen, and testes (Fig. 5B). For all four founder lines, the amount of Gα_{i2} in the fat and liver of mice that express the *pPCK-ASG*α_{i2} transgene was less than 5% of that observed for the control. In the kidney, the suppression of Gα_{i2} was more variable, some animals displayed less than 5% of the control amounts, others displayed wild-type amounts of expression. The variability of Gα_{i2} expression in the kidney may reflect epigenetic effects as a result of differences in the sites of integration of the transgene. These data do indicate, however, that Gα_{i2} expression was suppressed in target tissues. Furthermore, albeit low relative to the amount of endogenous *PEPCK* mRNA, the amount of Gα_{i2} antisense RNA that accumulated was sufficient to suppress Gα_{i2} subunit expression.

A major characteristic of the mice carrying the *pPCK-ASG*α_{i2} transgene was a failure to thrive (Figs. 6, A and B). Although similar to the controls at birth, after 6 weeks of postnatal development and antisense RNA expression, the transgenic mice without Gα_{i2} displayed >30% reduction in body weight. Food consumption was equivalent for control and transgenic mice, yet the difference in body weight of transgenic mice was still observed at 18 weeks of age, and plateaued at >20% below normal at 24 weeks. As a percentage of body weight, fat mass was reduced in the transgenic animals lacking Gα_{i2} (Fig. 6C). Although 30% smaller in body weight at 6 weeks of age, transgenic mice had liver mass equivalent to normal mice on a percent body weight basis. By 18 weeks of age, however, transgenic mice had lower body weights than normal mice, and a liver mass

Table 1. Tissue weights (g) of targeted and non-targeted tissues in normal and pPCK-ASGα_{12} transgenic BDF1 mice. Transgenic mice were produced and bred at the Stony Brook Transgenic-Mouse facility. Necropsy and histology was performed by Charles River Laboratories. The results displayed are mean values ± SEM (n = 6).

Tissue	Age (weeks)					
	6 Transgenic/normal	Ratio	12 Transgenic/normal	Ratio	18 Transgenic/normal	Ratio
Brain	0.39 ± 0.01/0.44 ± 0.03	0.89	0.42 ± 0.01/0.43 ± 0.01	0.98	0.45 ± 0.02/0.46 ± 0.02	0.98
Fat*†	0.09 ± 0.03/0.27 ± 0.03	0.33	0.19 ± 0.01/0.37 ± 0.04	0.49	0.19 ± 0.01/0.47 ± 0.01	0.40
Heart	0.11 ± 0.01/0.13 ± 0.01	0.85	0.14 ± 0.02/0.14 ± 0.01	1.00	0.19 ± 0.02/0.20 ± 0.02	0.95
Kidney*	0.14 ± 0.03/0.19 ± 0.02	0.74	0.19 ± 0.02/0.19 ± 0.02	1.00	0.28 ± 0.02/0.28 ± 0.03	1.00
Liver*	1.07 ± 0.08/1.49 ± 0.02	0.72	1.08 ± 0.04/1.49 ± 0.03	0.72	1.24 ± 0.03/1.89 ± 0.09	0.66
Lung	0.13 ± 0.01/0.15 ± 0.03	0.87	0.17 ± 0.02/0.18 ± 0.01	0.94	0.18 ± 0.02/0.19 ± 0.04	0.95
Sk. muscle‡	0.10 ± 0.02/0.15 ± 0.01	0.67	0.14 ± 0.02/0.14 ± 0.02	1.00	0.20 ± 0.05/0.22 ± 0.03	0.91

*Denotes target tissue for pPCK-ASGα_{12}. †Epididymal fat pad. ‡Gastrocnemius skeletal muscle.

considerably less (~20%) than that of the control on a percentage of body weight basis (Fig. 6C). Thus, the consequences of the loss of $G\alpha_{i2}$ on metabolic and developmental processes were observed in fat, but not liver at 6 weeks of age, whereas by 18 weeks of age the loss of $G\alpha_{i2}$ affected growth in both tissues.

The RNAase protection assays indicated that the steady-state accumulation of the transgene RNA was ~100-fold lower than that of the endogenous *PEPCK* mRNA. We offer two explanations for this observation. (i) A proposed mechanism of action for antisense RNA is to reduce the amount of mRNA available for translation by targeting the antisense RNA–mRNA duplex for degradation. (ii) The hybrid *pPCK-ASG*α_{i2} RNA may be less stable than the endogenous *PEPCK* mRNA and therefore not accumulate to equivalent levels. Our ability to detect antisense $G\alpha_{i2}$ RNA in liver but not in kidney nor fat tissues of the transgenic mice with the sensitive reverse transcription and PCR amplification assay may reflect the limited extent to which the antisense RNA accumulates in fat and kidney even when transcribed from a gene under the control of the *PEPCK* promoter.

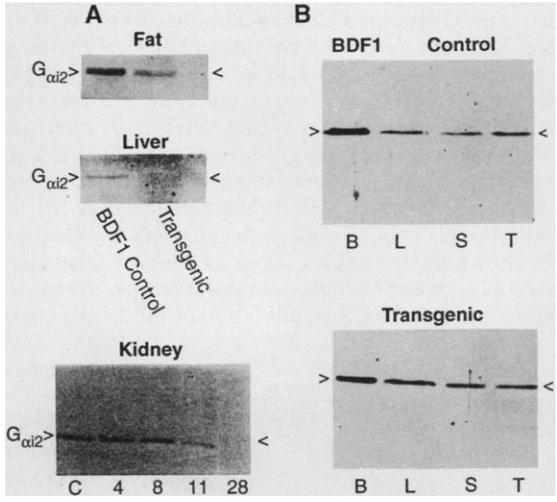

Fig. 5. $G\alpha_{i2}$ expression is suppressed in pPCK-ASGα_{i2} transgenic mice. Crude membranes were prepared from the indicated tissues obtained from both control and transgenic mice ranging in age from 6 to 18 weeks. Samples were subjected to SDS–polyacrylamide gel electrophoresis and transferred to nitrocellulose for immunoblot analysis with antibodies specific for $G\alpha_{i2}$ (CM-112). (**A**) $G\alpha_{i2}$ immunoblot of crude membranes (200 μg/lane) prepared from targeted tissues for pPCK-ASGα_{i2} expression. Lanes labeled from left to right in kidney samples are C (control BDF1) and transgenic mouse lines 4, 8, 11, and 28. The photographs shown for fat and liver samples are representative of $G\alpha_{i2}$ expression in all of the transgenic animals tested over four generations. (**B**) $G\alpha_{i2}$ immunoblot of crude membranes (30 μg/lane) prepared from non-targeted tissues isolated from control and transgenic mice. Lanes labeled from left to right in each blot are B, brain; L, lung; S, spleen; and T, testes.

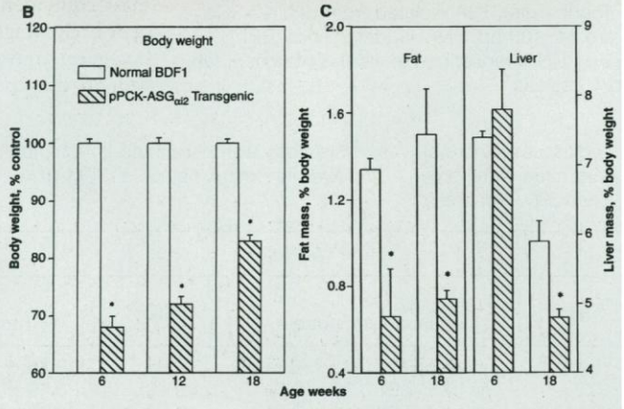

Fig. 6. Suppression of $G\alpha_{i2}$ expression by RNA antisense to $G\alpha_{i2}$ blunts neonatal growth. (**A**) The pPCK-ASGα_{i2} transgenic animals have a marked reduction in neonatal growth. Shown are control (left) and transgenic (right) male mice at 6 weeks of age. The body weights of the normal and transgenic mice shown were 17 g and 9.9 g, respectively. (**B**) Normal and transgenic mice (n = 6) were weighed at the times indicated after birth. Mice were then transported to the Charles River Laboratories for complete necropsy and histological examinations of targeted and non-targeted tissues. Fat mass (expressed as percent body weight) was significantly reduced in transgenic mice at 6 and 18 weeks of age. (**C**) Liver mass (as percent of body weight) was significantly reduced in transgenic mice at 18, but not 6 weeks. The values reported are expressed as mean ± SEM. Litter size of the transgenic mice (seven to nine pups) was not significantly different from the litter sizes of BDF1 control mice.

These results address a question relating the specificity of the effects observed in the transgenic mice to suppression of $G\alpha_{i2}$ and not to aberrant *PEPCK* gene expression resulting from integration of the transgene. The extremely low, steady-state accumulation of the transgene RNA relative to the *PEPCK* mRNA suggests that any pPCK-ASGα_{i2} transgene product would not contribute significantly to the PEPCK protein pool. Furthermore, results from RNAase protection assays demonstrate that the endogenous *PEPCK* mRNA is highly abundant and inducible by cAMP in both stably transfected FTO-2B cells as well as in hepatocytes and adipocytes from pPCK-ASGα_{i2} transgenic animals, demonstrating that the transgene does not affect endogenous *PEPCK* gene expression. The elevated steady-state accumulation of endogenous *PEPCK* mRNA that we observed in the pPCK-ASGα_{i2} transgenic mice likely reflects the elevation of intracellular cAMP, secondary to the suppression of $G\alpha_{i2}$. The reduction in $G\alpha_{i2}$ amounts observed in the adipose tissue of pPCK-ASGα_{i2} transgenic mice was associated with a threefold elevation in basal amounts of cAMP (4.99 ± 0.44 and 16.45 ± 1.37 pmol per 10^5 cells for control and transgenic mice, respectively), as well as the loss of the inhibitory adenylylcyclase response in isolated fat cells (*16*).

G protein–linked responses regulate many cellular processes in vivo such as the hormonal regulation of metabolic pathways such as lipolysis, glycogenolysis, and gluconeogenesis. The G proteins G_s and G_i regulate these pathways by altering the activity of adenylylcyclase and hence the intracellular amounts of cAMP. G_s and G_i have also been implicated in oncogenesis and differentiation. Constitutively active mutants of $G\alpha_s$ and $G\alpha_{i2}$ subunits have been identified in pituitary, thyroid, ovarian, and adrenal tumors (*7*, *17*, *18*). $G\alpha_s$ and $G\alpha_{i2}$ also regulate adipogenesis in mouse 3T3-L1 cells (*19*) and stem cell differentiation of F9 teratocarcinoma cells into primitive endoderm (*20*), in a manner that cannot be explained simply by changes in intracellular cAMP.

Here, suppression of $G\alpha_{i2}$ in liver and fat of transgenic mice was associated with a dramatic reduction in neonatal growth. The reduction in body mass cannot be explained by the reduction in the mass of targeted organs, nor by differences in food consumption, suggesting that a reduction in $G\alpha_{i2}$ expression induces a metabolic alteration ad-

versely affecting neonatal growth. Thus, the blockade of the expression of a single G protein subunit, $G\alpha_{i2}$, in tissues prominent in metabolism, affects not only the development of targeted tissues, but can also result in pleiotropic metabolic consequences.

REFERENCES AND NOTES

1. L. Birnbaumer, J. Abramowitz, A. M. Brown, *Biochim. Biophys. Acta* **1031**, 163 (1990).
2. H. R. Bourne, D. A. Sanders, F. McCormick, *Nature* **348**, 125 (1990).
3. H. R. Bourne, D. A. Sanders, F. McCormick, *Nature* **349**, 117 (1991).
4. A. G. Gilman, *Adv. Second Messenger Phosphoprotein Res.* **24**, 51 (1990).
5. W. F. Simonds *et al.*, *Proc. Natl. Acad. Sci. U.S.A.* **86**, 7809 (1989).
6. F. R. McKenzie and G. Milligan, *Biochem. J.* **267**, 391 (1990).
7. J. Lyons *et al.*, *Science* **249**, 655 (1990).
8. Y. Hod and R. W. Hanson, *J. Biol. Chem.* **263**, 7747 (1988).
9. J. Liu *et al.*, *ibid.* **266**, 19095 (1991).
10. J. P. Garcia Ruiz, R. Ingram, R. W. Hanson, *Proc. Natl. Acad. Sci. U.S.A.* **75**, 4189 (1978).
11. F. J. Ballard and R. W. Hanson, *Biochem. J.* **104**, 866 (1967).
12. C. M. Moxham, Y. Hod, C. C. Malbon, unpublished material.
13. C. M. Moxham and C. C. Malbon, unpublished material.
14. J. R. Hadcock, M. Ros, D. C. Watkins, C. C. Malbon, *J. Biol. Chem.* **265**, 14784 (1990).
15. C. M. Moxham, Y. Hod, C. C. Malbon, unpublished material.
16. C. M. Moxham and C. C. Malbon, *Dev. Genet.*, in press.
17. C. A. Landis *et al.*, *Nature* **340**, 692 (1989).
18. E. Clementi, N. Malagaretti, J. Meldolesi, R. Taramelli, *Oncogene* **5**, 1059 (1990).
19. H-y. Wang, D. C. Watkins, C. C. Malbon, *Nature* **358**, 334 (1992).
20. A 235-bp Nhe I–Sst I fragment containing the 39 nucleotides corresponding to the $G\alpha_{i2}$ antisense sequence was excised from the vector pLNC-AS$G\alpha_{i2}$ [D. C. Watkins, G. L. Johnson, C. C. Malbon, *Science* **258**, 1373 (1992)]. The protruding ends were made flush. The blunt-ended fragment was engineered into the first exon of the rat *PEPCK* gene at the Bgl II site (position +69 relative to the transcription start site) with standard recombinant DNA techniques. Prior to insertion of the antisense sequence into the Bgl II site, the rat *PEPCK* gene was subcloned as two separate fragments into the vector pGEM −7Zf(+); a 1.0-kb EcoR I–Hind III fragment and a 5.8-kb Hind III–Bam HI fragment. The 1.0-kb fragment contained the Bgl II insertion site. Plasmids carrying the desired orientation of the insert were selected by DNA sequencing. After insertion, the two fragments were religated with standard techniques. To discriminate between the endogenous *PEPCK* gene and the transgene, primers (P1, P2) were synthesized that were complementary to the flanking ends of the insert, thus permitting subsequent PCR amplification of only the 235-bp insert present in the pPCKAS$G\alpha_{i2}$ construct. A physical map of the rat *PEPCK* gene was reported previously [E. G. Beale *et al.*, *J. Biol. Chem.* **260**, 10748 (1985)]. The sequence of the primers P1 and P2 was 5′-CGTTTAGTGAACCGTCAGA-3′ and 5′-TTGCCAAACCTACAGGTGGG-3′, respectively. The 460 bp of 5′-flanking promoter sequences within the construct contained the responsive elements necessary for the tissue-specific, hormonal, and developmental regulation of gene expression, as observed with the endogenous *PEPCK* gene [M. M. McGrane *et al.*, *ibid.* **263**, 11443 (1988); M. M. McGrane *et al.*, *J. Biol. Chem.* **265**, 22371 (1990)].
21. B. L. Brown, J. D. M. Albano, R. P. Elkins, A. M. Sghzeri, *Biochem. J.* **121**, 561 (1971).
22. B. Hogan, F. Constantini, E. Lacy, *Manipulating the Mouse Embryo* (Cold Spring Harbor Laboratory, Cold Spring Harbor, NY, 1986) pp. 174–175.
23. C. M. Moxham and C. C. Malbon, unpublished material.
24. W. Richards and S. Strickland, unpublished material. Briefly, 1 μg of genomic tail DNA was added to a 50-μl reaction volume containing the following: 25 pmol of each primer, 200 μM each of dATP, dTTP, dCTP, dGTP, 0.4% Triton X-100, 0.3% NP-40, 1.5 units of Taq polymerase, 50 mM KCl, 10 mM tris-HCL (pH 8.8), 1.5 mM $MgCl_2$. The PCR amplification was performed according to the Perkin-Elmer Cetus protocol for the *Hot Start* technique with Ampliwax PCR gems.
25. All animals were handled in accordance with the guidelines established by the Institutional Animal Care and Use Committee at SUNY/Stony Brook.

26. We thank Dr. F. Yan Ling for her invaluable help with the production of the transgenic mice. Supported by grants from the NIH (C.C.M.), American Heart Association (C.C.M.) and Weight Watchers Foundation (C.C.M.).

23 November 1992; accepted 10 March 1993

Cue-Invariant Shape Selectivity of Macaque Inferior Temporal Neurons

Gyula Sáry, Rufin Vogels,* Guy A. Orban

The perception of shape is independent of the size and position of the shape and also of the visual cue that defines it. The same shape can be recognized whether defined by a difference in luminance, by motion, or by texture. Experiments showed that the shape selectivity of individual cells in the macaque inferior temporal cortex did not vary with the size and position of a shape and also did not vary with the visual cue used to define the shape. This cue invariance was true for static luminance and texture cues as well as for relative motion cues—that is, for cues that are processed in ventral and dorsal visual pathways. The properties of these inferior temporal cells meet the demands of cue-invariant shape coding.

Recently, it has been shown that the direction selectivity of cells in the primate extrastriate middle temporal area (MT) is generally form-cue–invariant (*1*). This may underlie the form-cue invariance in the perception of motion direction. Here, we present neurophysiological evidence that a population of cells in the macaque inferior temporal cortex (IT) (*2*) forms the neural correlate of a different type of perceptual invariance: the visual cue invariance of shape perception (*3*) (Fig. 1).

Neuropsychological observations in humans as well as in animals have shown that IT lesions cause severe impairments in visual shape discrimination (*4*). Also, single-cell recording studies have revealed that the responses of IT cells can be highly selective for visual shape, preferring some shapes over others (*5*, *6*). It has been shown that IT neurons keep their shape selectivity irrespective of changes in retinal image size, contrast sign, or position (*7*). These neuronal response invariances match the invariance in size, contrast, and position of shape perception, which suggests that the IT is involved in the processes that underlie the recognition of shapes and objects. These experiments have used shapes defined by a single visual cue, luminance contrast. We stimulated IT cells using shapes defined by one of three visual cues and determined whether their shape selectivity was cue-independent.

Neurons were recorded in the IT cortex of two male rhesus monkeys performing a fixation task (*8*). Sets of eight figures (Fig. 2) created by random dots were used as stimuli (*9*). Each figure could be defined by one of three cues: luminance difference, relative motion, or texture difference (Fig. 1). In the case of the luminance-defined

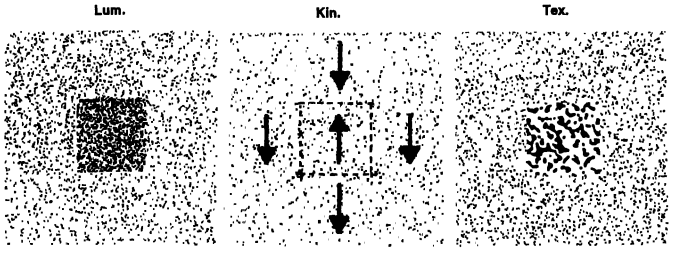

Fig. 1. Shape perception is cue-invariant. A square can be defined by a difference in luminance between figure and background (Lum.), by relative motion of the dots (up versus down) of the figure and background (Kin.), or by a difference in dot size (texture) between figure and background (Tex.). For the middle figure (Kin.), the arrows show the direction of motion of the dots and the hatching indicates the virtual borders, which are rendered visible solely by virtue of relative dot motion.